Current Science
CS 6 (1), 5833-5845 (2026)
Received 07 January 2026 | **Accepted 12 February** 2026 | **Online Available 14 February** 2026
https://doi.org/10.52845/CS/2026-6-1-14

Current Science
Current Science

OPEN ACCESS
ISSN(O) 2795-8639

Original Article

Pectin-Functionalized Magnetic Nanoadsorbent for Efficient Mn^{2+} Removal and Reuse

Yilin Wang

Senior High School Department, Soong Ching Ling School, No. 2, Yehui Road, Qingpu District, Shanghai City, China

***Corresponding Author: Yilin Wang**

Abstract:
To address the environmental pollution caused by Mn^{2+}-containing industrial wastewater, this study successfully synthesized a novel, efficient, and magnetically separable composite adsorbent by Immobilizing natural biomass pectin onto the surface of aminated core-shell magnetic nanoparticles (Fe3O4@SiO2@NH2). This study systematically investigated the adsorption behavior and desorption-regeneration performance of this material for Mn2+ in wastewater, aiming to provide theoretical and experimental basis for its practical application.
The composite magnetic nanocomposite adsorbent exhibited excellent Mn^{2+} adsorption performance under optimal conditions (dosage 10.0 mg, adsorption time 6.0 h, solution pH 6.0). In 20.0 mL of 100.0 mg/L Mn2+ solution, its removal efficiency reached 78.02%, and the equilibrium adsorption capacity was as high as 156.03 mg/g. Furthermore, the adsorbent demonstrated outstanding reusability, with a desorption efficiency of 90.04% in the first cycle, highlighting its great potential for practical applications.
Keywords: Pectin, Fe3O4@SiO2@NH2, Composite nano-magnetic adsorbent, Mn2+ solution, Adsorption-regeneration

1. Research Background

In recent years, the presence of "green" technologies has been increasing: electric vehicles (EVs) drive by silently on the roads, and an increasing number of charging stations are being installed in residential areas. New energy vehicles (NEVs) are integrating into my daily life at an unprecedented speed. However, a critical issue closely related to daily living has also emerged: the ultimate fate of the batteries from these EVs after they are retired (or decommissioned). Literature and media reports indicate that if these spent batteries are not handled properly, the internal electrolytes and chemicals may leak, causing contamination to water, air, and soil. Significantly, they contain substantial quantities of valuable heavy metals such as nickel, cobalt, and manganese. If disposed of improperly, this would constitute a significant waste of resources. This issue, stemming from real-life observations, inspired my interest in inquiry.

Among these heavy metals, manganese (Mn) warrants particular attention. Although manganese is an essential trace element for maintaining normal physiological functions, excessive exposure induces toxicity. Chronic or excessive exposure to manganese may cause initial symptoms such as dizziness and fatigue, in severe cases, it may lead to neurological disorders resembling Parkinson's disease (manganism) [1-3]. Additionally, manganese is the fourth most widely used metal in industry. Its applications are extensive, including the production of glass, ceramics, adhesives, welding materials, paints, gasoline anti-knock additives, and batteries.

Therefore, developing cost-effective technologies to treat Mn-containing industrial wastewater is not only vital for resource recovery but also critical for safeguarding public health.

Currently, conventional technologies for treating heavy metal wastewater include chemical precipitation, physical adsorption, and biological methods [4]. Among them, adsorption is favored for its simplicity, cost-effectiveness, and high efficiency. The efficacy of this technology relies on the availability of high-performance material. However, traditional adsorbents such as activated carbon and zeolites generally suffer from limitations such as low adsorption capacity and challenging recovery and regeneration. Many novel adsorbents reported in recent years are hindered by complex synthesis processes, high costs, or unsatisfactory performance, limiting their potential for large-scale industrial application. Therefore, developing novel adsorbent that are abundant, low-cost, environmentally friendly, and highly efficient remains a primary research focus and difficulty.

Among various candidate materials, pectin has emerged as a promising biomass adsorbent. Primarily, pectin offers distinct environmental and economic advantages. As a ubiquitous polysaccharide found in plant cell walls—particularly in agricultural by-products such as citrus peels and apple pomace—pectin is widely available, cost-effective, and biodegradable. Structurally, pectin possesses inherent properties that make it an effective adsorbent. Its polymeric chain is abundant in active functional groups, specifically carboxyl (-COOH) and hydroxyl (-OH) groups. These functional groups facilitate the effective binding of heavy metal ions from aqueous solutions via electrostatic attraction and chelation mechanisms [5-7]. However, native pectin is subject to limitations, including high water solubility, poor mechanical strength, and challenges in post-adsorption separation and recovery. While pectin effectively complexes metal ions, integrating it with magnetic materials significantly enhances its adsorption efficiency and separability. Therefore, the inherent limitations of pectin can be overcome by developing composite materials that leverage the synergistic properties of their components.

To address the aforementioned limitations of pectin, this study proposes innovative solution: fabricating a composite of pectin and magnetic nanoparticles [8-10]. $Fe_3O_4@SiO_2@NH_2$ was selected as the magnetic core to enable rapid separation and recovery under an external magnetic field, effectively overcoming the challenge of pectin retrieval. By immobilizing pectin onto the surface of the magnetic core, the objective was to synthesize a novel composite material that synergizes the advantages of both components: utilizing the abundant adsorption sites of pectin for efficient Mn^{2+} removal, and leveraging the magnetic core for convenient separation and recycling. While magnetic pectin composites have been successfully applied to the adsorption of Pb^{2+} and Cu^{2+} in previous studies [11-13], the novelty of this work lies in the systematic application of this technology to the specific environmental challenge of Mn^{2+} pollution derived from spent lithium batteries. This study aims to experimentally validate this concept and provide a promising technical solution for resource recovery.

2. Research Process

2.1 Materials and Equipment

2.1.1 Materials and Reagents

The main chemical reagents used in this study are shown in Table 2-1.

Table 2-1 Main Experimental Materials

Name	Specification	Source Manufacturer
Low-ester Pectin	Food Grade	Xinjiang Fufeng Biotechnology Co., Ltd.
0.1M Sodium Hydroxide	AR	Fludau

Aminated Silica-coated Magnetic Beads	100nm	Jiangsu Zhichuan Technology
Calcium Chloride	AR	Sinopharm Reagent
Anhydrous Sodium Carbonate	AR	Shanghai Zhanyun Chemical Co., Ltd.
Sodium Dodecylbenzenesulfonate	AR	Sinopharm Reagent
Manganese Chloride	AR	damas-beta
Sodium Hydroxide	AR	Sinopharm Reagent
Hydrochloric Acid	AR	Sinopharm Reagent

2.1.2 Instruments and Equipment

The main instruments and equipment used in this study are shown in Table 2-2.

Table 2-2 Main Instruments and Equipment

Name	Model	Brand
Analytical Balance	BSA224S	Shanghai Lichen Instrument Co., Ltd.
Magnetic Stirrer	MS3	JOANLAB
Ultrasonic Cleaner	SB-120D	Ningbo Xinzhi Biotechnology Co., Ltd.
Magnet	30mm×5mm	Cilibao
Vacuum Drying Oven	DZF-6090	Shanghai Yiheng Scientific Instrument Co., Ltd.
pH Meter	100pro	Shanghai Lichen Instrument Co., Ltd.
Water Bath Constant Temperature Shaker	DKZ-2B	Shanghai Jinghong Experimental Equipment Co., Ltd.
Fourier Transform Infrared Spectrometer	Nicolet iS20	Thermo Fisher Scientific
Scanning Electron Microscope (SEM)	ZEISS Sigma 300	ZEISS
Nanoparticle and Zeta Potential Analyzer	Nano ZS90	Malvern (UK)
Inductively Coupled Plasma Optical Emission Spectrometer (ICP-OES)	Avio	PerkinElmer

2.2 Experimental Process

2.2.1 Preparation of Composite Nano-magnetic Adsorbent

(1) Pretreatment of Pectin Solution (Saponification): First, a pivotal pretreatment step —saponification—was performed on the pectin raw material. Low-ester pectin (1.0 g) was dissolved in 60 mL of 0.1 M NaOH solution and reacted under rapid stirring at 50°C for 1 h. The objective of this saponification was to hydrolyze methyl ester groups (-$COOCH_3$) in the pectin molecules under alkaline conditions, thereby exposing more active carboxyl groups (-COO^-). These groups serve as key binding sites for the subsequent adsorption of metal ions. Throughout the process, nitrogen gas was introduced to create an inert atmosphere, as polysaccharides are susceptible to oxidative degradation under thermal and alkaline conditions. This nitrogen protection effectively prevented oxidation, thereby maintaining the integrity of the molecular structure.

(2) Dispersion of Magnetic Particles: Aminated silica-coated magnetic particles (1.0 g) were weighed and ultrasonically dispersed in

ultrapure water to prevent aggregation.

(3) Cross-linking and Compositing: Subsequently, the two solutions were mixed and ultrasonicated again to ensure uniform dispersion. A $CaCl_2$ solution was then added dropwise in a water bath at 40–60°C. The Ca^{2+} ions acted as a cross-linking agent. These ions simultaneously bind to -COO^- groups on adjacent pectin chains, forming stable "egg-box" structures (ionic bridges). This process immobilized the pectin network onto the surface of the magnetic particles, yielding a structurally stable composite material.

(4) Post-treatment: After the reaction, the product was magnetically separated, washed repeatedly with distilled water until neutral, vacuum-dried at 50°C, ground, and stored for further use. Notably, during the initial preparation, the high viscosity of the saponified pectin solution caused aggregation, posing a challenge to uniform mixing. This issue was resolved by optimizing the stirring rate and enhancing the ultrasonic dispersion, thereby ensuring the uniformity of the product.

2.2.2 Characterization of Composite Nano-magnetic Adsorbent

(1) Fourier Transform Infrared Spectroscopy (FT-IR): This technique was employed to identify the surface chemical functional groups, confirming the successful grafting of pectin onto the magnetic particles.

(2) Scanning Electron Microscopy (SEM): SEM was utilized to characterize the microscopic morphology of the material, specifically to assess surface roughness and porosity, which correlate with the abundance of adsorption sites.

(3) Zeta Potential Analysis: This analysis was conducted to measure the surface charge under varying pH conditions, thereby elucidating the mechanism of electrostatic interaction between the material and ions.

2.2.3 Mn^{2+} Adsorption Experiment

To determine the optimal adsorption conditions, an L9(3^3) orthogonal array design was employed in this study. Three key factors were investigated: adsorbent dosage (A), adsorption time (B), and initial solution pH (C). The specific levels for each factor are listed in Table 2-3. All adsorption experiments were conducted using 20 mL of Mn^{2+} solution (100 mg/L) and agitated at 150 rpm in a constant-temperature water bath shaker. Following adsorption, the adsorbent was magnetically separated, and the residua Mn^{2+} concentration in the supernatant was quantified using an Inductively Coupled Plasma Optical Emission Spectrometer (ICP-OES). The optimal adsorption parameter combination was determined using the removal efficiency and adsorption capacity as evaluation indicators.

Table 2-3 Orthogonal Experiment Design Table

Experimental Level	A Dosage / mg	B Time / h	C pH
1	10.0	2.0	4.0
2	15.0	4.0	6.0
3	20.0	6.0	8.0

2.2.4 Mn^{2+} Desorption and Regeneration Experiment

To evaluate the reusability of the adsorbent, desorption and regeneration experiments were conducted. In initial attempts, the regeneration efficiency was suboptimal, and the desorption efficiency was very low, raising concerns

regarding the stability of the material. It was hypothesized that the poor performance resulted from an improper selection of the eluent or insufficient contact time. Consequently, different concentrations of EDTA solution were systematically evaluated as the eluent. EDTA can form stable complexes with Mn^{2+}, theoretically allowing it to sequester Mn^{2+} from the adsorbent via competitive chelation. Through comparative experiments (specific results in section 3.5), optimal elution conditions were established. Subsequently, multiple "adsorption-desorption" cycles were performed under these conditions to comprehensively evaluate its regeneration performance.

2.3 Calculation of Adsorption and Regeneration Function Indicators

(1)Adsorption Performance Indicators

The removal efficiency and equilibrium adsorption capacity of the adsorbent for Mn^{2+} were calculated by formulas (1) and (2), respectively:

$$R(\%)=\frac{(C_0-C_e)}{C_0}\times 100 \quad (1)$$

Where C_0 represents the initial concentration of Mn^{2+} (mg/L); C_e denotes the equilibrium concentration of Mn^{2+} (mg/L).

$$Q_e(\mathrm{mg/g})=\frac{(C_0-C_e)V}{m} \quad (2)$$

where V is the volume of the solution (L), and m is the mass of the adsorbent (g).

(2) Regeneration Performance Indicator

The desorption efficiency was calculated using Equation (3) :

$$D(\%)=\frac{C_d\times V_d}{(C_0-C_e)\times V}\times 100 \quad (3)$$

Where C_d is the concentration of Mn^{2+} in the eluent (mg/L), and V_d is the volume of the eluent (L). (C_0 and C_e are defined as above).

3 Results and Discussion

3.1 Fourier Transform Infrared Spectroscopy Characterization

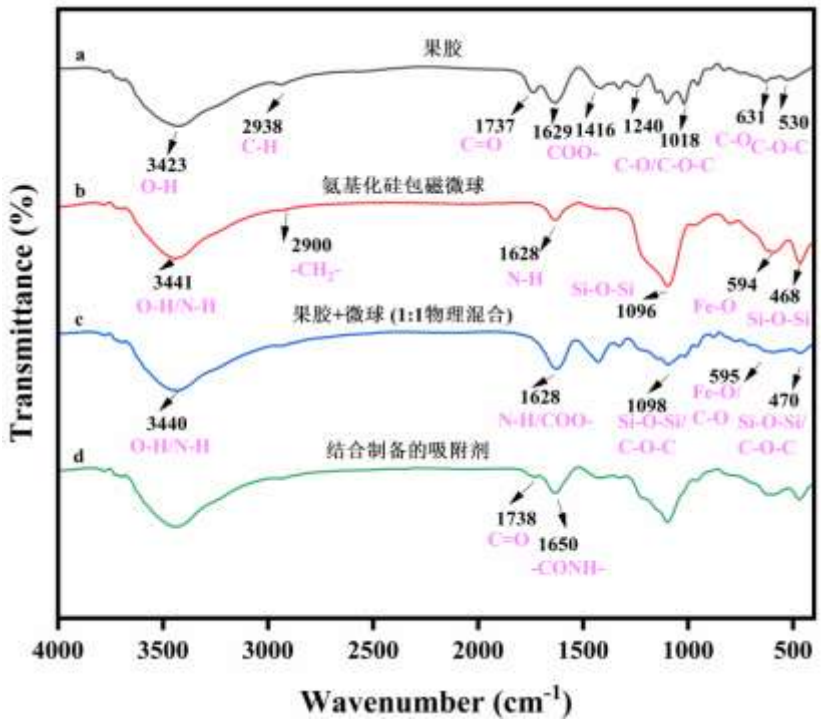

Figure 3-1 FT-IR spectra of different materials

To verify the successful synthesis of magnetic nanocomposite adsorbent, the raw materials (pectin, aminated silica-coated magnetic beads), their physical mixture, and the final product were characterized using FT-IR (Figure 3-1). Curve a shows the spectrum of pure low-ester pectin. Typical polysaccharide broad absorption peaks typical of polysaccharides were observed at ~3423 cm^{-1} (O-H stretching vibration) and ~2938 cm^{-1} (C-H stretching vibrations), along with complex C-O-C and C-O vibration peaks in the fingerprint region (1000-1200 cm^{-1}). The sharp absorption peak at 1737 cm^{-1} is attributed to the C=O stretching vibration of esterified carboxyl groups (-$COOCH_3$), while the absorption peaks at 1629 cm^{-1} and 1416 cm^{-1} correspond to the asymmetric and symmetric stretching vibrations of free carboxyl groups (-COO^-), respectively. Curve b represents the spectrum of the aminated silica-coated magnetic nanoparticles. Strong absorption peaks at ~594 cm^{-1} and ~468 cm^{-1} correspond to the vibrations of Fe-O bonds and Si-O-Si bonds, respectively, confirming the Fe_3O_4@SiO_2 core structure. The Si-O-Si asymmetric stretching vibration peak at ~1096 cm^{-1} further confirms the presence of the silica coating. The absorption peak at ~1628 cm^{-1} is assigned to the N-H bending vibration, indicating the successful surface amination. Curve c displays the spectrum of the physical mixture of pectin and magnetic nanoparticles. This spectrum is basically a simple linear superposition of the characteristic peaks of the two, and no new chemical bonds were observed. Conversely, in the spectrum of final composite adsorbent (Curve d), the most significant change is the appearance of a new shoulder peak at ~1650 cm^{-1}. Located between the -COO^- asymmetric stretching vibration of pectin and the N-H bending vibration of the amino group, this peak is assigned to the C=O stretching vibration (amide I band) in the newly formed amide bond (-CONH-). The formation of this new chemical bond provides direct evidence of the condensation reaction between the carboxyl groups on the pectin molecular chain and the amino groups on the surface of the magnetic particles. This confirms that the pectin was successfully grafted onto the surface of the magnetic particles via covalent bonding, rather than simple physical adsorption.

3.2 SEM Characterization

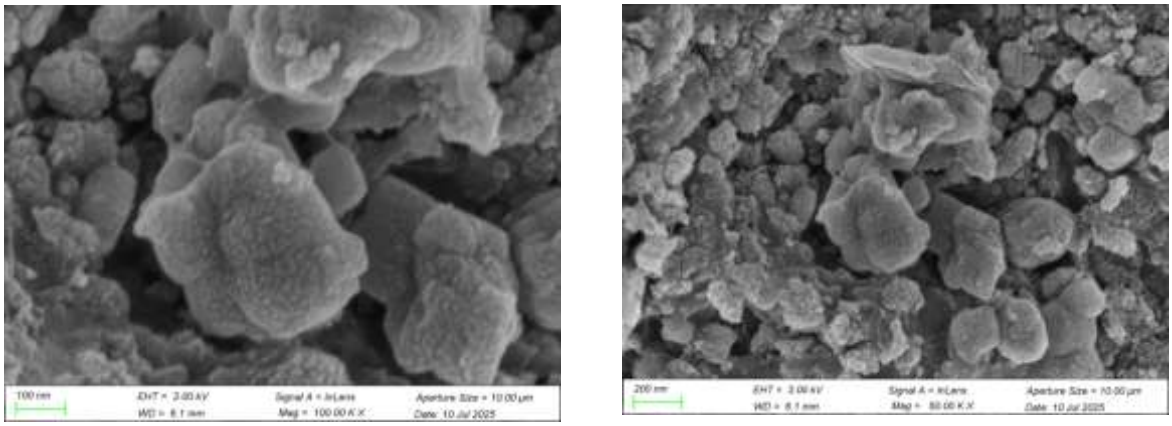

Figure 3-2 SEM images of composite nano-magnetic material

The surface morphology of the magnetic nanocomposite adsorbent was characterized via SEM (Figure 3-2). Low- and high-magnification images reveal that the synthesized particles exist as near-spherical aggregates with relatively uniform size distributions. Rather than exhibiting a smooth surface, the particles display a highly rough and uneven texture characterized by abundant folds, grooves, and micropores. This complex three-dimensional porous architecture

significantly enhances the effective specific surface area, thereby increasing the availability of active sites for the subsequent adsorption process. This unique surface structure is the structural foundation for high-efficiency adsorption, indicating the material's promising potential for practical applications.

3.3 Zeta Potential Characterization

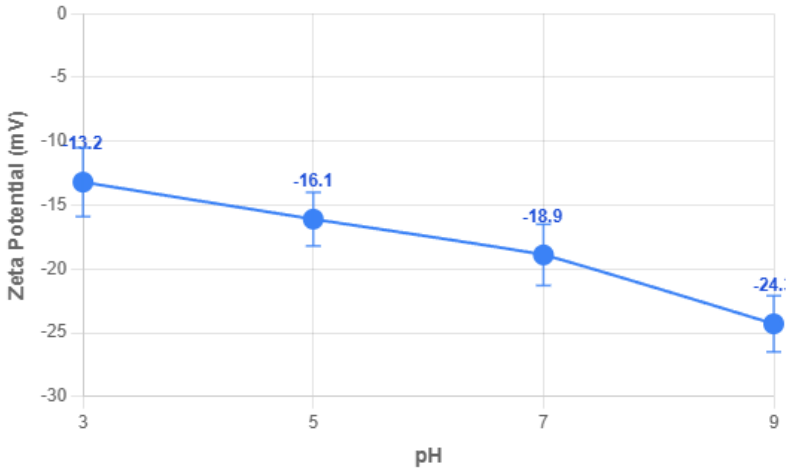

Figure 3-3 Zeta potential of adsorbent at different pH conditions

To investigate the influence of pH value on the surface charge properties of the adsorbent, Zeta potential measurements were conducted. The adsorbent was ultrasonically dispersed into a series of buffer solutions (pH 3.0, 5.0, 7.0, and 9.0) to obtain uniform suspensions. Samples were subsequently analyzed using a nanoparticle and Zeta potential analyzer, with results shown in Figure 3-3. The results show that within the investigated pH range, the material surface remained negatively charged, with Zeta potential values decreasing (becoming more negative) as pH increased. This trend is attributed to the deprotonation of abundant acidic functional groups (mainly -COO^-) on the material surface at higher pH levels. These groups facilitate the capture of positively charged Mn^{2+} ions via strong electrostatic attraction. Mechanistically, this implies that higher pH conditions favor adsorption **Error! Reference source not found.Error! Reference source not found.Error! Reference source not found.**. However, determining the optimal pH requires balancing surface charge with metal ion speciation to prevent $Mn(OH)_2$precipitation at excessively high pH, which could confound adsorption results.

3.4 Orthogonal Experiment

3.4.1 Analysis of Orthogonal Experiment Adsorption Rate under Different Adsorption Conditions

To systematically optimize the adsorption process parameters, the study used the L9(3^3) orthogonal experiment method to investigate three key factors: adsorbent dosage, adsorption time, and solution pH.

Table 3-1 Visual Analysis of Orthogonal Experiment Adsorption Rate

Exp. No.	A	B	C	Adsorption Rate/%
1	10.0	2.0	4.0	69.48
2	10.0	4.0	8.0	59.78
3	10.0	6.0	6.0	79.76
4	15.0	2.0	8.0	61.44

5	15.0	4.0	6.0	86.23
6	15.0	6.0	4.0	69.93
7	20.0	2.0	6.0	81.17
8	20.0	4.0	4.0	71.33
9	20.0	6.0	8.0	63.73
K_1	69.7	70.7	70.2	—
K_2	72.5	72.4	82.4	—
K_3	72.1	71.1	61.7	—
R	2.9	1.7	20.7	—
Order of Influence	pH > Dosage > Time			
Optimal Combination	Dosage 15.0mg, Time 4.0h, pH 6.0 ($A_2B_2C_2$)			

When using adsorption rate as the evaluation criterion, magnitude of influence of each factor was evaluated based on the range (R).. As presented in Table 3-1, R(pH) = 20.7 >> R(Dosage) = 2.9 > R(Time) = 1.7, indicating that the solution pH was the most significant factor affecting the Mn^{2+} adsorption rate, followed by dosage, while time exerted the minimal influence. This finding aligns with the analysis results of the Zeta potential in section 3.3, i.e., a higher pH (pH 6.0, K_2=82.4) can provide a stronger driving force .for electrostatic attraction. Based on the K value analysis, the theoretical optimal combination was determined to be $A_2B_2C_2$.

3.4.2 Analysis of Orthogonal Experiment Unit Adsorption Capacity under Different Adsorption Conditions

Table 3-2 Visual Analysis of Orthogonal Experiment Adsorption Capacity

Exp. No.	A	B	C	Adsorption Capacity mg/g
1	10.0	2.0	4.0	138.96
2	10.0	4.0	8.0	119.56
3	10.0	6.0	6.0	159.52
4	15.0	2.0	8.0	81.92
5	15.0	4.0	6.0	114.97
6	15.0	6.0	4.0	93.24
7	20.0	2.0	6.0	81.17
8	20.0	4.0	4.0	71.33
9	20.0	6.0	8.0	63.73
K_1	139.3	100.7	101.2	—
K_2	96.7	102.0	118.6	—
K_3	72.1	105.5	88.4	—
R	67.3	4.8	30.1	—
Order of Influence	Dosage > pH > Time			
Optimal Combination	Dosage 10.0mg, Time 6.0h, pH 6.0 ($A_1B_3C_2$)			

Conversely,, when using unit adsorption capacity served as the evaluation criterion, the hierarchy of influence of the factors shifted. As shown in Table 3-2, R(Dosage) = 67.3 >> R(pH) = 30.1 > R(Time) = 4.8, indicating that the adsorbent dosage becomes the most critical factor affecting the adsorption capacity. This is because, with a fixed total amount of Mn^{2+}, increasing the adsorbent dosage enhances the total removal rate, but reduces the mass of Mn^{2+} adsorbed per unit mass of adsorbent, thus lowering the unit adsorption capacity. Based on the K value analysis, the theoretical optimal combination for

maximizing adsorption capacity was determined to be $A_1B_3C_2$.

3.4.3 Orthogonal Experiment Verification Experiment

Table 3-3 Orthogonal Experiment Verification Experiment

Condition Combination	Adsorption Rate %	Adsorption Capacity mg/g
$A_2B_2C_2$	85.69	114.25
$A_1B_3C_2$	78.02	156.03

To identify the optimal experimental conditions, verification experiments were conducted on the two theoretical combinations (Table 3-3). Results indicate that while $A_2B_2C_2$ combination could indeed achieve a higher removal rate, but its unit adsorption capacity was substantially lower than that of the $A_1B_3C_2$. In evaluating adsorbent performance, unit adsorption capacity is considered a superior indicator of intrinsic efficiency and economic viability. Therefore, to maximize material utilization while ensuring a high removal rate (78.02%), $A_1B_3C_2$ (Dosage: 10.0 mg; Time: 6.0 h; pH: 6.0) was ultimately established as the optimal adsorption condition. To objectively assess the performance of this adsorbent, its maximum adsorption capacity (156.03 mg/g) was compared with literature values for other adsorbents. t was found to be superior to common materials such as biochar and modified clay minerals. These comparative results demonstrate that the synthesized material possesses significant competitive advantages and promising application prospects for treating Mn-containing wastewater.

3.5 Desorption and Regeneration Experiment

3.5.1 Selection of Desorption Conditions

The economic viability and environmental sustainability of an adsorbent hinge on its effective regeneration and reusability. EDTA was selected as the eluent due to its strong chelating affinity for divalent metal ions. Figure 3-4 shows the desorption efficiency using varying concentrations of EDTA on Mn^{2+}. The desorption efficiency initially increased with EDTA concentration, peaking at 90.04% at 0.20M, before slightly declining. This indicates that this concentration of EDTA can effectively elutes the adsorbed Mn^{2+} from the material surface, thereby facilitating the regeneration of the adsorbent. Consequently, 0.20M was identified as the optimal desorption agent concentration for subsequent cycle experiments.

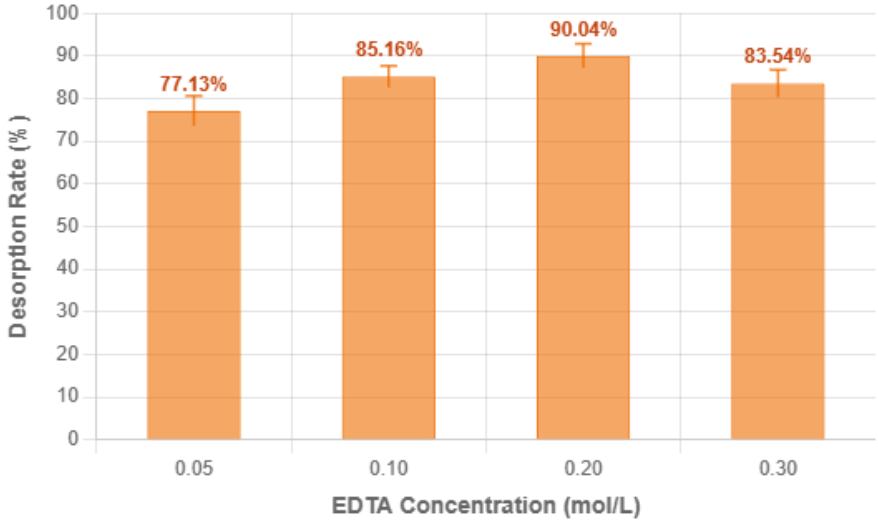

Figure 3-4 Adsorbent desorption effect at different EDTA concentrations

3.5.2 Cyclic Regeneration Experiment

The reusability of the adsorbent was investigated under optimal adsorption and desorption conditions (Figure 3-5). The results show that the composite adsorbent has favorable regeneration performance. In the first cycle, both the adsorption rate and desorption rate were excellent. However, as the cycle count reached four, both efficiencies exhibited a notable decline. The adsorption rate could remain at 62.44% after the second cycle, indicating moderate stability. The performance decline is likely attributed to the partial degradation or leaching of active components (such as pectin) from the material surface, as well as the irreversible occupation or blockage of some adsorption sites during repeated cycling [1Error! Reference source not found.]. Despite the decline, the adsorbent retained considerable adsorption-desorption capability, underscoring its potential as a reusable adsorbent for practical applications.

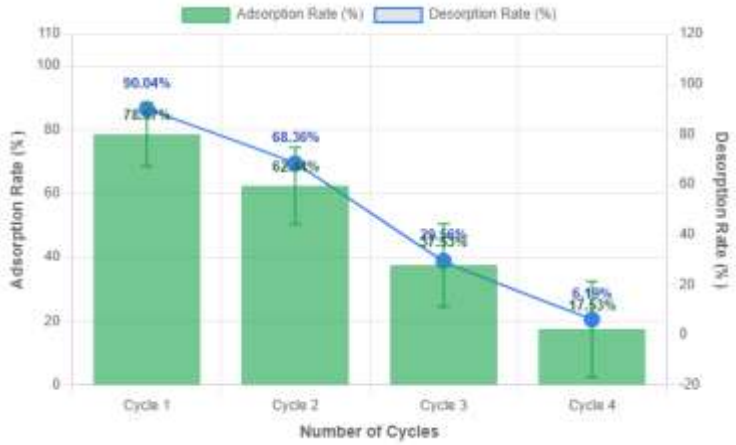

Figure 3-5 Adsorbent desorption effect at different cycle numbers

4 Conclusion and Outlook

This study successfully synthesized a pectin-functionalized core-shell magnetic nanocomposite adsorbent and systematically evaluated its Mn^{2+} adsorption behavior and regeneration performance. This work provides an efficient and eco-friendly strategy for treating heavy metal industrial wastewater. The main conclusions are as follows：

(1) Characterization via FT-IR and SEM confirmed that pectin was successfully grafted onto the surface of the aminated silica-coated Fe_3O_4 magnetic core via covalent bonds. The resulting core-shell composite exhibited a rough, porous morphology with a high specific surface area.

(2) Orthogonal experimental results indicated that under the optimal process parameters (adsorbent dosage 10.0 mg, adsorption time 6.0 h, initial solution pH 6.0), the unit adsorption capacity of the adsorbent for Mn^{2+} was as high as 156.03 mg/g. This performance is significantly superior to that of most biochar and modified clay mineral adsorbents reported in the literature.

(3) The composite adsorbent exhibited excellent magnetic response and cyclic regeneration capabilities. Considerable adsorption efficiency was retained after four adsorption-desorption cycles, demonstrating its potential for cost-effective practical applications.

While this study demonstrates the application potential of this material, bridging the gap between b

ench-scale research and industrial application req uires further investigation in the following areas:

(1) In-depth analysis and verification of adsorptio n mechanism: While this study confirmed the role of electrostatic attraction via Zeta potenti al analysis, specific chemisorption mechanism s, such as complexation or chelation between Mn^{2+} and the functional groups (e.g., -COO^{-}) —remain to be fully clarified. Future research should integrate adsorption modeling (thermo dynamics, kinetics, and isotherms) with advan ced spectral techniques, particularly X-ray ph otoelectron spectroscopy (XPS). These metho ds will facilitate the identification of atomic-le vel changes in elemental valence states and ch emical environments, ultimately enabling the construction of a comprehensive model syner gizing physisorption and chemisorption..

(2) Study on selective adsorption behavior in com plex media: Real-world industrial wastewater (particularly spent battery leachate) often cont ains a variety of coexisting cations. Coexistin g ions (such as Ni^{2+}, Co^{2+}, Ca^{2+}, Mg^{2+}) inevita bly compete for active sites, potentially inhibit ing Mn^{2+}adsorption.. Therefore, conducting m ulti-component competitive adsorption experi ments is crucial for evaluating selectivity and verifying the material's feasibility for precise pollutant removal in complex environments. F urthermore, density functional theory (DFT) c alculations should be employed to theoreticall y quantify interaction energies between metal ions and active sites, providing guidance for ta rgeted material design.

(3) Exploration of material's macroscopic configu ration and engineering application: The curren t nano-powdered adsorbent may face challeng es regarding mass loss during separation and h ydraulic issues (e.g., pressure drop) in practica l applications. Therefore, immobilizing the na no-adsorbent onto macroscopic carriers (such as hydrogels, porous foams, or fiber membran es) and conducting continuous-flow fixed-bed column experiments are essential steps toward industrialization. This will help to obtain key parameters necessary for engineering design, s uch as breakthrough curves and mass transfer zone lengths.

(4) Life Cycle Assessment (LCA): To ensure sust ainability, a comprehensive LCA should be co nducted covering the material's entire life cycl e—from preparation and application to dispos al. This assessment will evaluate environment al impacts and economic costs, providing a sci entific basis for developing genuinely green w ater treatment technologies.

Acknowledgements

Under the supervision of my advisors, this researc h was conducted primarily by me over a six-mont h period. Specifically, I independently executed th e synthesis of the magnetic nanocomposite, chara cterized the material (FT-IR, SEM, Zeta potential) , and conducted comprehensive performance testi ng. This included designing and executing the L9(3^3) orthogonal experiment, determining the maxi mum Mn^{2+}adsorption capacity, and performing fo ur cyclic regeneration experiments.

During the conceptualization phase, my superviso rs provided guidance on establishing the research direction. They offered critical review and sugges tions for the experimental design, particularly reg arding the orthogonal array. Furthermore, I receiv ed training in the operation of precision instrumen ts (ICP and Zeta potential analyzers) and benefite d from their academic guidance regarding peak as signments in infrared spectra, specifically for the newly emerged amide/ester peaks. During manusc ript preparation, my supervisors provided valuabl e feedback on the logical flow of the discussion a nd the overall structure.

Several technical challenges were encountered an d resolved during the research. For example, initia l experiments revealed that pectin tended to aggre gate in alkaline solutions, affecting reaction unifo rmity. This issue was mitigated by maintaining an

inert nitrogen atmosphere, enhancing agitation, an d optimizing water addition. Agglomeration of m agnetic nanoparticles in the aqueous phase was ov ercome by secondary ultrasonication and the addit ion of sodium dodecylbenzenesulfonate (SDBS) a s a dispersant. In regeneration experiments, desor ption efficiency initially declined significantly aft er the first cycle. Following systematic optimizati on, the use of 0.20 M EDTA combined with opti mized elution timing effectively enhanced the cyc lic stability.

Through this project, I acquired in-depth knowled ge of nanomaterial synthesis, characterization, an d environmental applications. More importantly, I honed my skills in independent experimental desi gn, data analysis, and scientific problem-solving. This experience has solidified my interest in scien tific research and reinforced my determination to pursue advanced studies in related fields.

References

1. Li, J.X., et al., *Evaluation and optimization of carbon reduction efficiency of recycling systems for retired ternary lithium batteries.* China Environmental Science, 2023. **43**(1): p. 9.
2. Teng, X.H., et al., *Threats of environmental manganese pollution to biological health.* Journal of Northeast Agricultural University, 2021. **52**(1): p. 90-96.
3. He, X., et al., *Health effects of manganese exposure.* Frontier of Medicine & Pharmacy, 2017. **7**(8): p. 3.
4. Wang, X.Y., *Preparation of pectin-modified magnetic nanomaterial adsorbents and their application in heavy-metal removal*. 2012, Hunan University.
5. Xiao, C. and C.T. Anderson, *Roles of pectin in biomass yield and processing for biofuels.* Front Plant Sci, 2013. **4**: p. 67.
6. Jonassen, H., et al., *Preparation of ionically cross-linked pectin nanoparticles in the presence of chlorides of divalent and monovalent cations.* Biomacromolecules, 2013. **14**(10): p. 3523-31.
7. Sharma, R. and M. Ahuja, *Thiolated pectin: Synthesis, characterization and evaluation as a mucoadhesive polymer.* Carbohydrate Polymers, 2011. **85**: p. 658-663.
8. Yang, M., Y.P. Hu, and J. Li, *Advances in the application of surface-modified Fe3O4 magnetic nanoparticles in pesticide and veterinary drug residue detection.* Guangdong Chemical Industry, 2017. **44**(12): p. 2.
9. Chen, S., et al., *Preparation of acrylamide-modified pectin-Fe3O4 magnetic microspheres and their adsorption properties for Cu2+ in water and seafood.* Journal of Chinese Institute of Food Science and Technology, 2019. **19**(3): p. 6.
10. Zhang, J.G., et al., *Synthesis of polyethyleneimine–carboxymethyl cellulose and its adsorption properties for metal ions.* Polymer Materials Science and Engineering, 2014. **30**(3): p. 15-20.
11. Huang, H., et al., *Preparation and adsorption properties of pectin–chitosan composite magnetic microspheres.* Journal of Neijiang Normal University, 2014. **29**(10): p. 5.
12. Hu, D.W., et al., *Preparation of modified pectin-Fe3O4 magnetic microspheres and their adsorption properties for Pb2+*. Inorganic Salts Industry, 2020. **52**(6): p. 24-29.
13. Wan, J.F., et al., *Preparation of modified pectin-Fe3O4 magnetic microspheres and studies on their adsorption properties for Cu2+*. Research and Application of Chemistry, 2018. **30**(5): p. 765-772.